This full text paper was peer reviewed at the direction of IEEE Communications Society subject matter experts for publication in the ICC 2007 proceedings.

Quantifying the Interference Gray Zone in Wireless Networks: A Measurement Study

Wonho Kim*, Jeongkeun Lee*, Taekyoung Kwon*, Sung-Ju Lee†, and Yanghee Choi*

*School of Computer Science and Engineering, Seoul National University, Korea
†Mobile and Media Systems Lab, Hewlett-Packard Labs, Palo Alto, USA
Email: whkim@mmlab.snu.ac.kr, jklee@mmlab.snu.ac.kr, tkkwon@snu.ac.kr, sjlee@hp.com, yhchoi@snu.ac.kr

***Abstract*—In wireless networks where communications are made over a shared medium, interference and collisions are the primary causes of packet drops. In multi-hop networks such as wireless mesh networks, due to the hidden terminal problem, limiting the effects of collisions and interference is a key in achieving high performance. Typical wireless medium access control protocols perform carrier sensing to avoid collisions. Most research efforts so far has used the binary model when studying carrier sensing and interference; a node is either carrier sensed or not, and a link is either interfered or not. In reality however, there exists a gray zone. Carrier sensing and interference should be represented in continuous values. Using the measurement data from our 802.11a wireless mesh network test-bed, we propose metrics that represent the levels of carrier sensing and interference. Using our metrics, we also propose methods to estimate broadcast throughput and goodput. We evaluate the accuracy of our methods by comparing our models with the measured data. In addition, we investigate the impact of the capture effect on interference.**

I. Introduction

Wireless networks continue to grow in popularity and deployment. Most people use wireless networks, both wireless LAN and cellular communications, in their daily routine. Office networks, home networks, and community networks are typical examples of WLAN we use. As the advanced communication technologies emerge, we seek high speed connectivity in addition to reliability. Because communications in wireless networks are made over a shared medium, interference and collisions are the primary causes of packet drops. In multi-hop networks such as wireless mesh networks, due to the hidden terminal problem, limiting the effects of collisions and interference is a key in achieving high performance.

In order to avoid interference and collisions, typical wireless medium access control protocols perform carrier sensing. Understanding and modeling the behavior of carrier sensing and interference is a key in achieving high performance in WLANs. Most research efforts [1]–[4] so far however, has used the binary model when studying carrier sensing and interference; a node is either carrier sensed or not, and a link is either interfered or not. In reality however, there exists a gray zone. For example, in our 10 node 802.11a wireless mesh network test-bed, 18% of the node pairs are within the CS gray zone. Moreover, we found that the range of the interference gray zone exceeds 12 dB. Therefore, carrier sensing and interference should be represented in continuous values.

In this paper, we quantify the levels of carrier sensing and interference into a metric using the measurement data from our 802.11a wireless network test-bed. For carrier sensing, from the measurement result, we set the throughput thresholds for the carrier sensing degrees of 0 (i.e., no carrier sensing) and 1 (complete carrier sensing). We use the goodput thresholds for interference degree. For the values in between (i.e., the gray zone), we utilize the SNR difference between the packets sent by the two senders to calculate the metric. This metric formation is based on our measurement observation that the broadcast throughput and goodput degrade linearly as the signal strength from an interferer increases.

Using our metrics, we also propose methods to estimate broadcast throughput and goodput between two wireless flows. Using our metrics, we estimate the packet transmission rate and the portion of lost packets to predict the effective broadcast goodput. We evaluate the accuracy of our methods by comparing our models with the measured data. In addition, we investigate the impact of the capture effect on interference.

The rest of this paper is organized as follows: Section II describes the wireless mesh network test-bed and the measurement setup. Section III discusses physical carrier sensing in 802.11a, its continuous nature of it, and a simple estimation model to predict broadcast transmission throughput. Similarly, Section IV describes interference in 802.11a, an estimation model to predict broadcast reception goodput, and the capture effect. Section VI concludes this paper.[2]

II. Testbed Setup

In order to study the effect of the carrier sensing (CS) and interference mechanisms, we measure the broadcast transmission (TX) throughput and reception (RX) goodput in the 802.11a mesh test-bed. A test-bed node is a single-board

This work was supported in part by Hewlett-Packard Laboratories University Relations Program and the Brain Korea 21 project of the Ministry of Education, Korea.

[2]We distinguish between the throughput at a sender and the goodput at a receiver. Throughput is defined as the rate of bytes transmitted at the sender's application whereas goodput is defined as the rate of bytes received at the receiver's application. In the presence of interference, reception goodput is less than transmission throughput.

1-4244-0353-7/07/$25.00 ©2007 IEEE

Authorized licensed use limited to: Seoul National University. Downloaded on February 10, 2009 at 23:42 from IEEE Xplore. Restrictions apply.

computer [5] equipped with a single mini-PCI 802.11a card using Atheros chipset [6]. As for CS mechanism used in our test-bed, Atheros chipset uses a combination of some indicators such as Automatic Gain Control (AGC) unlock indicator and Energy Detect (ED) indicator [7].

We use UDP broadcast traffic to study the behavior of CS and interference and remove the effects of 802.11 unicast MAC mechanisms (i.e., exponential backoff and retransmissions) and TCP mechanisms (i.e., end-to-end retransmissions and congestion control). The application on each node continuously generates UDP packets of 1,000 bytes and sends them out to a broadcast address to make its link layer output queue non-empty. The used PHY rate is 6 Mbps which is the basic rate in the IEEE 802.11a.[3] Each broadcast session lasts for 15 seconds and we measure 10 sessions whose average value is plotted. We set up a CS relation between the two nodes by adjusting the antenna, transmission power, and node placement. We use two antennas for each node to facilitate antenna adjustment: one for transmission and the other for reception.

III. Carrier Sensing

In this section, we describe physical carrier sensing in 802.11 systems and present a metric to quantify it. Based on the measurement results from the wireless mesh network test-bed, the carrier sensing thresholds are given for the proposed metrics. In addition, we suggest a simple method to predict broadcast TX throughput using the proposed CS metric.

A. Carrier Sensing in 802.11a

A wireless station withholds its transmission when it senses the carrier (channel) busy due to an ongoing transmission. The 802.11 systems employ two physical carrier sensing mechanisms: *preamble detection* and *energy detection* [8]. As each transmission begins with a unique preamble sequence, a node senses an ongoing transmission in the channel when it detects a preamble sequence. When the preamble portion is missed, a receiver still can sense the busy carrier when it detects any signal whose received signal strength is higher than the CCA (Clear Channel Assessment) sensitivity level. CCA affects the CS range. That is, if node S_2 is within S_1's CS range, S_1 can detect S_2's transmissions (see the example of Fig. 1). Note that in 802.11a systems, the CS range is smaller than the packet reception range which is similar to a preamble detection range. We presume that node S_2 does not sense node S_1's packet transmission when S_2 can not receive and decode the packet from S_1.

B. Carrier Sensing Metric

First, we measure the broadcast TX throughput of one node when there is no traffic from the other node. We observe the average throughput of 4.9968 Mbps with 0.01 Mbps standard deviation. The actual TX throughput is smaller than the nominal PHY rate because of the preamble, protocol encapsulation (header), interframe spacing time, and backoff time overhead.

[3]6 Mbps is also the lowest and the most robust bit rate in IEEE 802.11a.

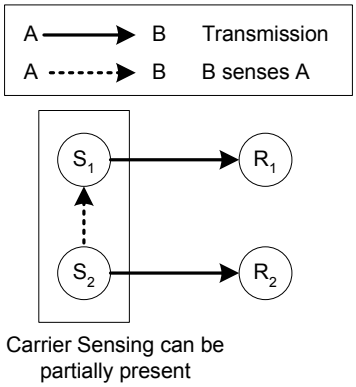

Fig. 1. Experimental setup for carrier sensing.

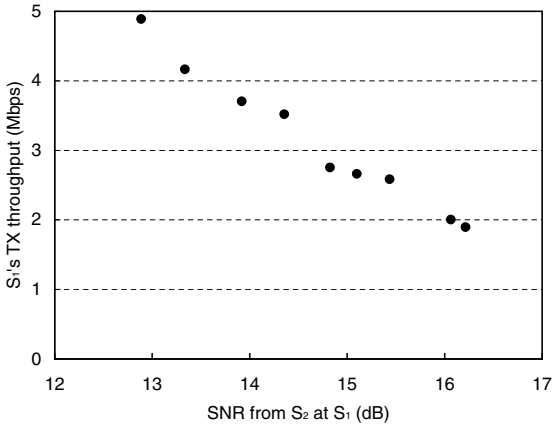

Fig. 2. The level of CS vs. SNR.

We hence call this actual TX throughput 5 Mbps as the *channel capacity* of 6 Mbps PHY rate.

We now measure the TX throughput of two nodes when both nodes transmit concurrently and sense each other's transmission. We obtained 2.65 Mbps TX throughput for each node. The sum of two nodes, 5.3 Mbps is larger than the 5 Mbps channel capacity, and is consistent with the observations from [9], [10]. The aggregate throughput initially increases as the number of nodes increases from one to a certain number (three or four), but then decreases as the number of nodes increases beyond that number. The initial throughput increase is due to the fact that backoff process is reduced when the number of nodes increases.

Observing the 802.11 operation in the test-bed, the CS value is not simply binary and is continuous. Node S_2 in Fig. 1 fails to sense S_1's transmission since its received signal strength is not larger than the CCA sensitivity level. In order to study the CS behavior, we measure the TX throughput of node S_1 while varying the S_2's transmission power over the range in which S_1 can sense S_2's transmission. The TX power of S_1 is fixed to a small value so that node S_2 cannot sense S_1's transmission.

Fig. 2 shows the broadcast TX throughput of node S_1 as the received signal strength of packets transmitted from S_2 to S_1 is

Authorized licensed use limited to: Seoul National University. Downloaded on February 10, 2009 at 23:42 from IEEE Xplore. Restrictions apply.

varied. Recall that S_2 is transmitting packets continuously. In our test-bed hardware, the signal strength is reported in terms of Signal-to-Noise-Ratio (SNR). When the SNR of packets from S_2 at S_1 is smaller than 13 dB, S_1 does not sense S_2's transmission and S_1 utilizes the full channel capacity (5 Mbps). Because S_2's packet is hardly received at S_1 when the SNR is below 13 dB, the plotting in Fig. 2 begins at 13 dB. As the SNR increases beyond 13 dB, S_1 senses more packets from S_2 and its TX throughput decreases until it reaches 2.0 Mbps when the SNR value is about 16 dB. A number of different node pairs are selected and examined in our test-bed, and we obtained similar results. We hence conclude that the CS gray zone appears between two SNR thresholds. We believe that these threshold values may depend on the 802.11a chipset vendor.

We have two CS thresholds (SNR_{low}=13 dB and SNR_{high}=16 dB) and define a CS metric $c_{S_1}(S_2)$ which refers to the degree of CS at S_1 for the signals transmitted from S_2 as follows

$$c_{S_1}(S_2) = \begin{cases} 0 & \text{if } snr_{S_1}(S_2) \leq SNR_{\text{low}} \\ 1 & \text{if } snr_{S_1}(S_2) > SNR_{\text{high}} \\ \frac{snr_{S_1}(S_2) - SNR_{\text{low}}}{SNR_{\text{high}} - SNR_{\text{low}}} & \text{otherwise} \end{cases}$$

where $snr_{S_1}(S_2)$ denotes the SNR of packets from S_2 at S_1. Note that $c_{S_1}(S_2)$ is linearly proportional to $snr_{S_1}(S_2)$ in dB scale, which is observed in Fig. 2.

C. Broadcast Throughput Prediction

As an application of CS metric, we suggest a simple method to predict TX throughput using the metric. A sender defers its transmission when it senses the channel busy, and hence the TX throughput of the sender is directly affected by carrier sensing.

For simplicity, we consider broadcast TX throughput on two links. Since there is no reliability features for broadcast traffic (i.e., no retransmissions and subsequent backoffs), TX throughput of a link is not affected by whether packet transmissions are successful or not. Therefore, when predicting the broadcast TX throughput, we do not consider the effect of interference from the other link on the intended receiver.

Let T_{S_1} and T_{S_2} denote the throughputs of S_1 and S_2 in Fig. 1 respectively. T_{S_1} is determined by two CS metrics: $c_{S_1}(S_2)$ and $c_{S_2}(S_1)$. First, T_{S_1} is affected by $c_{S_1}(S_2)$ which represents the degree of CS at node S_1 for the signals transmitted from node S_2 since S_1 defers its transmission when it senses transmissions from S_2. In addition, $c_{S_2}(S_1)$ also has an effect on T_{S_1}. As $c_{S_2}(S_1)$ is getting closer to 0, T_{S_2} sends more packets. As S_2 sends more packets, T_{S_1} is further decreased because S_1 has less chances to win the channel and send packets. Therefore T_{S_1} is a function of two CS metrics: $c_{S_1}(S_2) and c_{S_2}(S_1)$.

$$\begin{aligned} T_{S_1} &= f(c_{S_1}(S_2), c_{S_2}(S_1)) \\ T_{S_2} &= f(c_{S_2}(S_1), c_{S_1}(S_2)) \end{aligned} \quad (1)$$

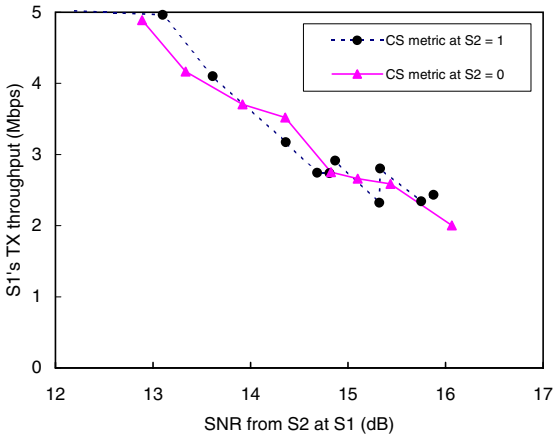

Fig. 3. TX throughput with different CS metric.

In order to study how TX throughput changes when different CS metrics are given, we measured two extreme cases. The first case is when $c_{S_2}(S_1)$ is fixed to 1, *the complete sensing state*, and $c_{S_1}(S_2)$ is changed from 0 to 1. The second case is when $c_{S_2}(S_1)$ is set to 0, *not sensing state*, and $c_{S_1}(S_2)$ is changed from 0 to 1. The results of those two cases are shown in Fig. 3. As shown in Fig. 3, two cases show similar patterns as $c_{S_1}(S_2)$ increases from 0 to 1. The differences between the throughput of the two cases are quite small, mostly less than 0.5 Mbps. We observe from these results that broadcast TX throughput is mainly determined by its own CS metric and not by the other sender's CS metric. Therefore, we propose a simple approximation to predict S_1's TX throughput considering only one CS metric, $c_{S_1}(S_2)$:

$$T_{S_1} = (1 - 0.5 \cdot c_{S_1}(S_2)) \cdot C_c \quad (2)$$

where C_c is the *channel capacity*, which is 5 Mbps in our test-bed. Likewise, T_2 is given by

$$T_{S_2} = (1 - 0.5 \cdot c_{S_2}(S_1)) \cdot C_c. \quad (3)$$

Using this simple estimation model, we investigate the accuracy of our model using the data from Fig. 3. The average and the standard deviation of the differences between the predicted throughput and the measured throughput are 0.46 Mbps and 0.18 Mbps for the $c_{S_2}(S_1)$=0 case. For the $c_{S_2}(S_1)$=1 case, the average is 0.43 Mbps and the standard deviation is 0.32 Mbps. The average difference is less than 10% of the channel capacity.

IV. Interference

To measure and quantify the degree of the interference between a link and an interferer, we present an interference metric based on our measurements from the test-bed. In addition, using our interference metric, we present a model that predicts the broadcast RX goodput when the sender and the interferer are hidden from each other.

Authorized licensed use limited to: Seoul National University. Downloaded on February 10, 2009 at 23:42 from IEEE Xplore. Restrictions apply.

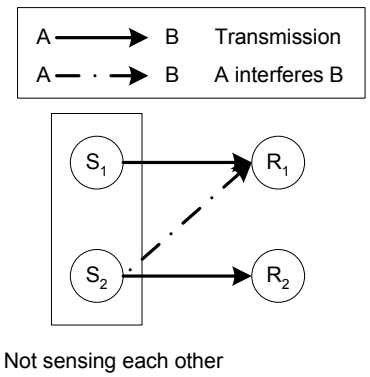

Fig. 4. Interference experimental setup.

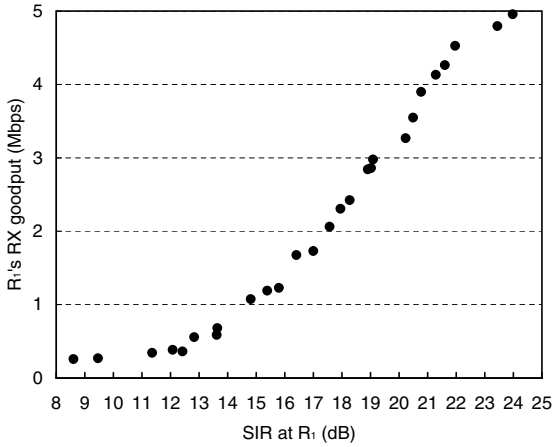

Fig. 5. Goodput of Link L_1 with varying degree of interference from S_2.

A. Interference in 802.11a

Interference occurs when packets transmitted by a sender are collided with and corrupted at a receiver by packets from another sender (i.e., interferer). In Fig. 4, when S_2 sends a packet to R_2 while a packet is transmitted from S_1 to R_1, those packets are collided at R_1 and can be lost, as S_2's transmission reaches R_1 because they are within the transmission range. We say that S_2 *interferes* the link from S_1 to R_1 in such a case.

In spite of collisions however, the receiver may successfully decode the received packet when Signal-to-Interference-and-Noise-Ratio (SINR) is higher than a certain level. Moreover, the degree of interference is not binary but has a continuous degree of impact on the reception of packets at the receiver according to the SINR value. We therefore present an interference metric using SINR measured at the receiver.

Interference occurs when either the sender or the interferer, or both are hidden from each other. In these cases, at least one of them fails to sense the transmissions from the other and transmits the packets even when there are ongoing transmissions. Packet collision occurs at the receiver in such cases. However, when both the sender and the interferer sense each other's transmissions, they will not send the packets at the same time, and no interference occurs. In this section, we focus on quantifying the degree of an interference when neither the sender or the receiver senses each other.

B. Interference Metric

In Fig. 4, when S_1 and S_2 transmit packets concurrently and S_2's transmission hinders R_1's successful reception of S_1's packets, we say link L_1 (from S_1 to R_1) is interfered by S_2. Interference occurs when SINR at R_1 goes below the required level. By ignoring the noise power which is usually much weaker than the intended signal (typically up to 70dB difference), the SINR becomes the Signal-to-Interference-Ratio (SIR). Most work in the literature models interference as binary: if the SIR at R_1 is below a threshold, S_2 effectively interferes R_1's reception of packets from S_1 and if the SIR is above the threshold, R_1's reception does not suffer interference from S_2.

Fig. 4 shows experimental setup for the interference measurement. Two senders S_1 and S_2 broadcast concurrently and continuously to one receiver R_1. We measure the goodput of received packets from S_1. The two senders are configured not to sense each other. The transmission power of interferer S_2 is varied to make R_1 experience various SIR values. The measurement results are plotted in Fig 5. It clearly shows that the interference in the reality exhibits a gray behavior between a complete interference state and a complete interference-free state. We also observe that the RX goodput increases almost linearly as the SIR increases.

Similar to the CS metric, we have two interference thresholds (SIR_{low}=12 dB and SIR_{high}=24 dB). Again, we believe that these threshold values may vary by chipset vendors. We define an interference metric $f_{L_1}(S_2)$ which quantifies the degree of interference at link L_1 (from S_1 to R_1) from the interferer S_2 as follows:

$$f_{L_1}(S_2) = \begin{cases} 1 & \text{if } sir_{L_1}(S_2) \le SIR_{\text{low}} \\ 0 & \text{if } sir_{L_1}(S_2) > SIR_{\text{high}} \\ \frac{SIR_{\text{high}} - sir_{L_1}(S_2)}{SIR_{\text{high}} - SIR_{\text{low}}} & \text{otherwise} \end{cases}$$

where $sir_{L_1}(S_2)$ is defined as "(SNR from S_1) *minus* (SNR from S_2) at R_1" in dB scale.

C. Broadcast Goodput Estimation

To predict the RX goodput, we need to consider the TX throughput of the sender as well as the interference. The amount of impact the interference has on the RX goodput is dependent on two factors: the degree of interference and the TX throughput of the interferer. The degree of interference can be modeled using the proposed interference metric. The second factor is the TX throughput of the interferer. Since we assume that the interferer does not sense the sender's transmissions, more packets sent from the interferer result in more packet collisions at the receiver, which consequently degrades the RX goodput of the link.

Broadcast RX goodput G_{L_1} of the link L_1 (from S_1 to R_1) in Fig. 4 is represented by a function

$$G_{L_1} = f(T_{S_1}, T_{S_2}, f_{L_1}(S_2)). \quad (4)$$

Authorized licensed use limited to: Seoul National University. Downloaded on February 10, 2009 at 23:42 from IEEE Xplore. Restrictions apply.

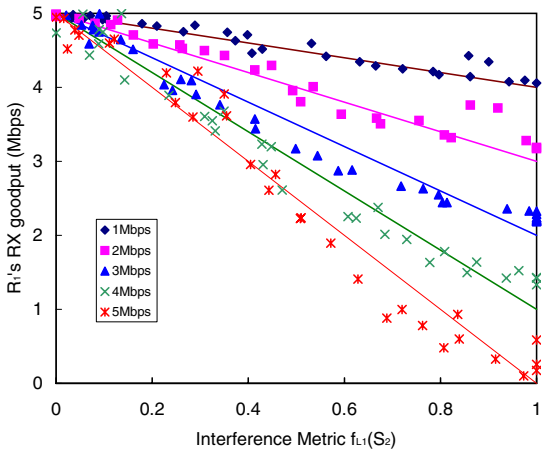

Fig. 6. RX goodput with different TX throughput of interferer.

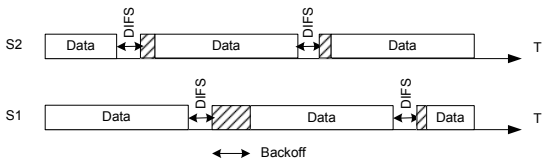

Fig. 7. Two links not sensing each other.

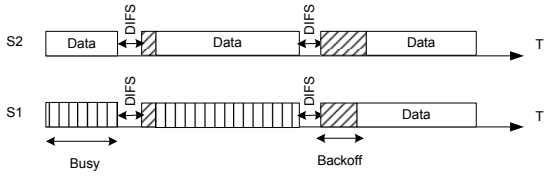

Fig. 8. Two senders with asymmetric CS relation.

The bit rate of packet collisions on link L_1 is approximated by

$$T_{col}(L_1) \approx T_{S_1} + T_{S_2} - C_c \tag{5}$$

where C_c is the *channel capacity* which is 5 Mbps in our test-bed. We can think of the interference metric $f_{L_1}(S_2)$ as a conditional probability that a packet cannot be decoded when it is collided at R_1. Therefore, the bit rate of lost packets on link L_1 is

$$T_{lost}(L_1) = T_{col}(L_1) \cdot f_{L_1}(S_2). \tag{6}$$

Then RX goodput G_{L_1} is given by

$$G_{L_1} = T_{S_1} - T_{lost}(L_1). \tag{7}$$

To validate the accuracy of the proposed estimation model, we measured RX goodput at the receiver with the various interference metric values. S_1 and S_2 are configured not to sense each other. The transmission power of the sender S_1 is fixed to a certain value and the transmission power of the interferer S_2 is varied to generate different SIR values at R_1. S_1 sends saturated traffic of 5 Mpbs and S_2 is set to transmit packets in the range from 1 Mbps to 5 Mbps. S_1 and S_2 are transmitting packets concurrently and R_1 receives packets from S_1.

Fig. 6 shows the RX goodput with the various interference metric values $f_{L_1}(S_2)$ when the interferer's Tx throughput changes from 1 Mbps to 5 Mbps. The five lines show the expected Rx goodputs from our estimation model and the plotted points represent measured Rx goodputs. Since a high interference metric value means high probability of packet corruptions, the RX goodput decreases linearly from T_{S_1} to (C_c - T_{S_2}) as the interference metric increases from 0 to 1. We compared our estimation model of RX goodput (the predicted goodput) to the measured goodput in Fig. 6. The average, median, and standard deviation of differences are 0.005, 0.004, and 0.227, respectively. These results show the high accuracy of our proposed model.

D. Capture Effect in Interference

The *capture effect* is the ability to receive a signal from one transmitter despite interference from another transmitter, even if the relative strengths of the two signals are almost the same. To make the capture effect happen notably, a *stronger packet*, a packet with higher signal strength, should come before a *weaker packet*, a packet with lower signal strength, because the radio locks onto the stronger packet and the weaker signal may not cause substantial interference. However, when the weaker packet arrives before the stronger packet, both packets are lost [11].

We first explain why the capture effect does not occur when the two senders are hidden from each other. Note that the senders are configured not to sense each other when measuring the effect of interference in Fig. 5. Fig 7 shows an example of the channel usage in such a case. Since DCF Inter Frame Spacing (DIFS) and backoff time is quite smaller than data packet transmission time, the portion of channel idle time is likely very small. As shown in Fig 7, most of the time a data packet transmission from S_1 begins when there already is an ongoing packet transmission from S_2. Therefore, a stronger packet from S_1 rarely arrives at R_1 when the channel is in the idle state. In order for the capture effect to occur, the stronger packet from S_1 should arrive at the receiver when it is in the idle state. Otherwise, the packet from S_2 hinders R_1 from synchronizing with the packet from S_1. When the receiver fails to synchronize with the stronger packet from S_1, packets from both the sender and the interferer are corrupted, unless the SIR is high enough to recover from such collisions.

Fig 8 shows a scenario in which the capture effect appear notably. In Fig 8, S_2 is configured not to sense S_1, but S_1 senses S_2. Here, a packet transmission from S_1 always begins prior to S_2's when the channel is in idle state because S_1 sends packets only when it wins the channel over S_2. That is, when S_1 senses S_2, R_1 always receives packets from S_1 prior to packets from S_2 whenever S_1 sends packets. In this scenario, the capture effect becomes effective. The radio at R_1 synchronizes with the packets from S_1 and thus R_1 decodes the packets from S_1 even with relatively strong interferences

Authorized licensed use limited to: Seoul National University. Downloaded on February 10, 2009 at 23:42 from IEEE Xplore. Restrictions apply.

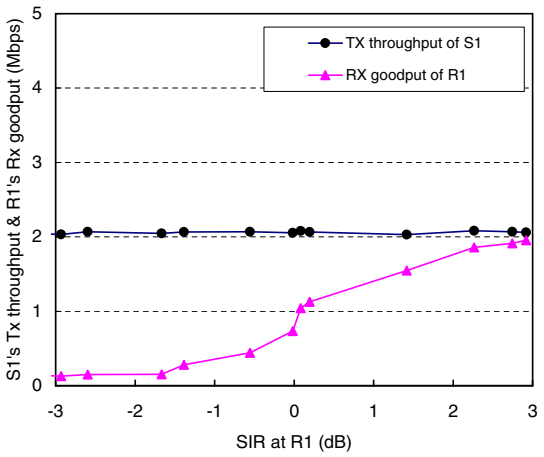

Fig. 9. SIR range with the capture effect.

from S_2 and low SIR at R_1.

The measurement results with the capture effect are shown in Fig. 9. Since S_1 senses S_2 but S_2 does not sense S_1, the TX throughputs of S_1 and S_2 are 2 Mbps and 5 Mbps, respectively. RX goodput measured at R_1 is close to zero when SIR is below -2 dB. However, RX goodput increases as SIR increases from -2 dB to +2 dB. It becomes almost equal to the TX throughput of S_1 when SIR is 2 dB or larger. We believe from these observations that the capture effect improves the link's utilization effectively since the required SINR threshold values are quite smaller compared to the ones in Fig. 5. In addition, the improvement is dependent on the CS relation between the sender and the interferer.

V. Related Work

The physical carrier sensing of 802.11 based multi-hop wireless networks has been studied by [3], [7]. Their experimental results and modeling provide a good insight on carrier sensing. However, the gray zone of carrier sensing is not discussed in any previous work. The SIR based interference model is a well studied subject (e.g. [4]), but they use binary modeling of interference. We have shown that interference should be represented in continuous values and the range of gray zone is considerably large (up to 12 dB). As the degree of interference exhibits a linearity with regard to the SIR value, the interference model can be extended to consider the gray zone based on the SIR value.

The gray zone of interference in wireless sensor networks is investigated in [12]. It found that the gray region appears due to the variation of SINR threshold and the threshold values are significantly dependent on the used hardware. We have shown however that interference exhibits a wide gray zone even when using a single hardware combination. Note also that we used 802.11 devices for our experiments instead of sensor communication devices.

Recent work [1], [2] has modeled the flow throughput with relation to carrier sensing and interference between flows. Their modeling can be extended to consider the gray zones of CS and interference by adopting our metrics.

VI. Conclusion

Understanding the behavior of carrier sensing and interference is critical in estimating and analyzing the performance of wireless networks. There has been a plethora of research effort to model carrier sensing and interference, and a simple binary model has been used in most cases. Using our 802.11a based wireless mesh network testbed measurements, we showed that the gray zone exists and presented metrics that quantify the degree of carrier sending and interference. Based on our proposed metrics, we devised models that predict the transmission throughput and received goodput. Our evaluation showed that our models show high accuracy. We have also investigated the impact of the capture effect on interference, and how we can exploit it to improve the channel capacity. Our future work includes extending our models to more than two flows.

References

[1] M. Garetto, J. Shi, and E. W. Knightly, "Modeling Media Access in Embedded Two-Flow Topologies of Multi-hop Wireless Networks," in *Proc. ACM MobiCom*, Cologne, Germany, Aug. 2005.
[2] M. Garetto, T. Salonidis, and E. W. Knightly, "Modeling Per-flow Throughput and Capturing Starvation in CSMA Multi-hop Wireless Networks," in *Proc. IEEE INFOCOM*, Barcelona, Spain, Apr. 2006.
[3] X. Yang and N. Vaidya, "On Physical Carrier Sensing in Wireless Ad Hoc Networks," in *Proc. IEEE INFOCOM*, Miami, FL, Mar. 2005.
[4] K. Jain, J. Padhye, V. Padmanabhan, and L. Qiu, "Impact of Interference on Multi-hop Wireless Network Performance," in *Proc. ACM MobiCom*, San Diego, CA, Sept. 2003.
[5] Soekris, Inc. http://www.soekris.com/.
[6] Atheros Communications, Inc. http://www.atheros.com/.
[7] K. Jamieson, B. Hull, A. Miu, and H. Balakrishnan, "Understanding the Real-World Performance of Carrier Sense," in *Proc. ACM SIGCOMM E-WIND Workshop*, 2005.
[8] IEEE 802.11a, *Part 11: Wireless LAN Medium Access Control (MAC) and Physical Layer (PHY) specifications: High-speed Physical Layer in the 5 GHz Band*, Supplement to IEEE Std. 802.11, Sept. 1999.
[9] S. Choi, K. Park, and C. Kim, "On the Performance Characteristics of WLANs: Revisited," in *Proc. of ACM SIGMETRICS*, Banff, Alberta, Canada, June 2006.
[10] T. Javidi, M. Liu, and R. Vijayakumar, "Saturation Rate in 802.11 Revisited," in *Annual Allerton Confercence on Communications, Control and Computing (Allerton 2005)*, Allerton, IL, Sept. 2005.
[11] K. Whitehouse, A. Woo, F. Jiang, J. Polastre, and D. Culler, "Exploiting the capture effect for collision detection and recovery," in *Proc. IEEE EmNetS-II*, Sydney, Australia, May 2005.
[12] D. Son, B. Krishnamachari, and J. Heidemann, "Experimental study of concurrent transmission in wireless sensor networks," in *Proc. ACM SenSys*, Boulder, CO, Nov. 2006.

Authorized licensed use limited to: Seoul National University. Downloaded on February 10, 2009 at 23:42 from IEEE Xplore. Restrictions apply.